

Fall of Spherical Particles through a Carreau Fluid*

P. DOLEČEK, H. BENDOŤA, B. ŠIŠKA, and I. MACHAČ**

*Department of Chemical Engineering, Faculty of Chemical Technology,
University of Pardubice, CZ-532 10 Pardubice
e-mail: Ivan.Machac@upce.cz*

Received 29 March 2004

Dedicated to the 80th birthday of Professor Elemír Kossaczky

Numerical solution of Hill's variational principles is presented for the estimation of upper and lower bounds to the drag coefficient correction function necessary for the determination of terminal velocity of spherical particles falling in purely viscous fluids obeying the four-parameter Carreau viscosity model. Some calculated data of the drag coefficient correction functions are compared with the corresponding experimental data. In the experiments, terminal falling velocities of spheres in aqueous solutions of polyalkylene glycol Emkarox HV 45 doped with a small amount (0.06 mass % and 0.08 mass %) of polyacrylamide Praestol 2935 were measured. At the same time, viscosity function measurements and oscillation dynamic tests of liquids were performed using rheometer RS 150 (Haake).

It was found that due to the liquid elasticity the experimental values X_{exp} of the drag coefficient correction function are beyond the calculated interval of upper and lower bounds and are higher than the upper bound X_u . However, terminal velocities of spheres falling in the test fluids with similar properties can be roughly estimated using the upper bound X_u for determination of a sphere drag coefficient.

Understanding the motion of particles falling in non-Newtonian fluids is not only of fundamental theoretical interest, but it is also of importance in many practical applications and industrial processes such as falling-ball viscometry, transport of slurries, sedimentation, fluidization, *etc.*

Therefore, great effort has been paid to investigation of the motion of spheres through non-Newtonian fluids over the last decades. At the same time, the fluid viscosity models containing zero shear viscosity should be preferred for describing the flow of purely viscous fluids around a sphere [1]. Such a widely used viscosity model (especially for polymeric liquids) is, for example, the Carreau model

$$\eta = \eta_{\infty} + (\eta_0 - \eta_{\infty}) \left[1 + (\lambda \dot{\gamma})^2 \right]^{\frac{m-1}{2}} \quad (1)$$

The creeping motion of spheres through a Carreau model fluid has been solved, for example, in the works [2–6]. Based on the Hill's variational principles, a problem for the numerical estimation of the upper and lower bounds to the drag coefficient correction function for the fall of spherical particles in fluids obeying

the Carreau viscosity model (1) was formulated in [5, 6]. The problem has been only solved for the dimensionless viscosity parameter

$$\eta_r = \frac{\eta_0 - \eta_{\infty}}{\eta_0} \quad (2)$$

encompassing the interval $1 \geq \eta_r \geq 0.96$. Here the Carreau model parameters η_0 and η_{∞} represent zero shear rate and infinity shear rate viscosities. Although for the creeping flow of a Carreau fluid usually $\eta_r \approx 1$, this quantity can acquire also lower values for some polymeric fluids. Therefore, the above-mentioned problem was recalculated extending the solution of Hill's variational principles for the interval $1 \geq \eta_r \geq 0.5$.

In this contribution, the obtained dependences of the upper bound X_u and the lower bound X_l on the dimensionless time parameter Λ and the Carreau model parameter m for selected values of η_r are presented. Some calculated data are compared with the corresponding experimental data X_{exp} , which were evaluated from measurements of terminal falling velocity of spherical particles moving in aqueous solutions

*Presented at the 31st International Conference of the Slovak Society of Chemical Engineering, Tatranské Matliare, 24–28 May 2004.

**The author to whom the correspondence should be addressed.

of polyalkylene glycol Emkarox HV 45 doped with a small amount of polyacrylamide Praestol 2935 under creeping flow conditions. These polymeric fluids satisfy the Carreau viscosity equation (1) and at the same time the value of parameter η_∞ is not negligible in comparison with η_0 .

THEORETICAL

Let us consider the free fall of a solid spherical particle in an unbounded purely viscous fluid the viscosity function of which is approximated by the Carreau viscosity model. Supposing the creeping flow conditions, the problem is described by the following set of equations:

continuity equation

$$\nabla \cdot \vec{u} = 0 \quad (3)$$

motion equation

$$\nabla p + \nabla \cdot \vec{\tau} - \rho \vec{g} = \vec{0} \quad (4)$$

and constitutive equation

$$\vec{\tau} = -2\eta \vec{\dot{\gamma}} \quad (5)$$

The non-Newtonian viscosity $\eta = \eta(II)$ is the function of the second invariant of the rate of deformation tensor defined as

$$II = \sqrt{\vec{\dot{\gamma}} : \vec{\dot{\gamma}}} \quad (6)$$

For the Carreau model liquid one gets

$$\eta = \eta_\infty + (\eta_0 - \eta_\infty) (1 + 2\lambda^2 II^2)^{\frac{m-1}{2}} \quad (7)$$

In spherical coordinates (r, θ, φ) , the dependent variables are the velocity components u_r, u_θ and the pressure p . The corresponding boundary conditions are given as

$$\text{for } r = R \quad u_r = u_\theta = 0 \quad (8)$$

$$\text{for } r \rightarrow \infty \quad u_r = u_t \cos \theta \quad (9)$$

$$u_\theta = -u_t \sin \theta$$

where R is the radius of the sphere, u_t is the terminal falling velocity.

The magnitude F_d of the drag force is obtained by integration of stresses acting on the sphere surface. It can be also expressed using the drag coefficient as

$$F_d = c_D \pi R^2 (1/2) \rho u_t^2 \quad (10)$$

At the same time, the drag coefficient for the flow of Carreau liquid around a sphere is given by

$$c_D = \frac{24}{Re_0} X \quad (11)$$

where the Reynolds number

$$Re_0 = \frac{2R u_t \rho}{\eta_0} \quad (12)$$

and X is the drag coefficient correction function.

The mathematical model given by eqns (3)–(12) can be approximately solved if it is replaced by an equivalent variational problem [7]. Following the development of *Slattery* for an Ellis model fluid [8], such variational problem, based on Hill's variational principles, has also been formulated for a Carreau model fluid [5, 6]. Solving this variational problem, the upper bound X_u and the lower bound X_l to the drag coefficient correction function X can be estimated.

Upper Bound to the Drag Coefficient Correction Function

Using the first (velocity) variational principle, the following relation has been derived for the correction function X [5]

$$\begin{aligned} X &= \frac{2}{3} \int_0^1 \int_{-1}^1 \eta_b II_b^2 x^{-4} dy dx \leq \\ &\leq \frac{2}{3} \int_0^1 \int_{-1}^1 E_b x^{-4} dy dx = \frac{2}{3} F_{ub} \end{aligned} \quad (13)$$

Here

$$x = R/r \quad (14a)$$

$$y = \cos \theta \quad (14b)$$

are the dimensionless spherical coordinates,

$$\begin{aligned} E_b &= \frac{ER^2}{\eta_0 u_t^2} = (1 - \eta_r) II_b^2 + \\ &+ \frac{\eta_r}{\lambda^2(1+m)} \left[(1 + 2\lambda^2 II_b^2)^{\frac{m+1}{2}} - 1 \right] \end{aligned} \quad (15)$$

is the dimensionless function E , which is for the Carreau liquid given as

$$\begin{aligned} E(II) &= \int_0^{II^2} \eta(II^2) dII^2 = \eta_\infty II^2 + \\ &+ \frac{\eta_0 - \eta_\infty}{\lambda^2(1+m)} \left[(1 + 2\lambda^2 II^2)^{\frac{m+1}{2}} - 1 \right] \end{aligned} \quad (16)$$

$$\eta_b = \frac{\eta}{\eta_0} \quad (17)$$

$$\lambda = \frac{\lambda u_t}{R} \quad (18)$$

are the dimensionless viscosity and dimensionless time parameters,

$$II_b = \frac{IIR}{u_t} = \left\{ \frac{3}{2}x^4 \left[y^2 \left(\frac{df}{dx} \right)^2 + \frac{1}{12}x^2(1-y^2) \left(\frac{d^2f}{dx^2} \right)^2 \right] \right\}^{\frac{1}{2}} \quad (19)$$

is the dimensionless second invariant of the rate of deformation tensor.

In order to express the invariant II_b , a trial velocity distribution must be specified that satisfies the continuity eqn (3) and the boundary conditions (8) and (9). The continuity equation will be fulfilled, if the nonzero velocity components are written in terms of stream function

$$u_r = -\frac{1}{r^2 \sin \theta} \frac{\partial \psi}{\partial \theta} \quad (20)$$

$$u_\theta = \frac{1}{r \sin \theta} \frac{\partial \psi}{\partial r} \quad (21)$$

At the same time, the stream function can be expressed by the following relationship

$$\psi = -\frac{1}{2}u_t r^2 \sin^2 \theta f(x) \quad (22)$$

In this study the calculations were performed using the function

$$f(x) = 1 - \frac{3}{2}x^a + \frac{1}{2}x^{3a} \quad (23)$$

In this case $\left(\frac{df}{dx} \right)_{x=1} = 0$, $f(1) = 0$, $f(0) = 1$, and $\lim_{x \rightarrow 0} x \frac{df}{dx} = 0$ so that also the boundary conditions are fulfilled. At the same time, if $a = 1$, the velocity distribution corresponds with Stokes solutions for the creeping flow of a Newtonian fluid past a sphere.

The optimum value of the parameter a in the function $f(x)$ can be determined by the minimization of the functional F_{ub} . The estimation of the upper bound X_u to the correction function $X = X(m, \Lambda, \eta_r)$ then follows from the relation (13).

Lower Bound to the Drag Coefficient Correction Function

According to the second (stress) variational principle, the following relation is valid [5]

$$X \geq \frac{1+m}{3} \int_0^1 \int_{-1}^1 E_b x^{-4} dy dx \geq \frac{1+m}{3} F_{lb} \quad (24)$$

The functional F_{lb} is given by the relationship

$$F_{lb} = - \int_0^1 \int_{-1}^1 E_{cb} x^{-4} dy dx + 2B \quad (25)$$

where the function

$$E_{cb} = 2\eta_b II_b^2 - E_b \quad (26)$$

can be determined by solving the equation

$$II_{\tau b} = 2\eta_b II_b \quad (27)$$

Here $II_{\tau b}$ is the dimensionless second invariant of the extra stress tensor. In order to express this invariant, a trial stress distribution that satisfies the motion eqn (4) must be specified. Using the following approximations of the extra stress tensor components [5, 8]

$$\tau_{r\theta} = B \frac{\eta_0 u_t}{R} x^4 \sin \theta \quad (28)$$

$$\tau_{\theta\theta} = \tau_{\varphi\varphi} = -\frac{1}{2}\tau_{rr} = B \frac{\eta_0 u_t}{R} (x^2 - x^4) \cos \theta \quad (29)$$

one gets

$$II_{\tau b} = B \left\{ 2x^4 \left[x^4 (1-y^2) + 3(1-x^2)^2 y^2 \right] \right\}^{\frac{1}{2}} \quad (30)$$

The optimum value of the parameter B can be determined by the maximization of the functional F_{lb} . The estimation of the lower bound X_l to the correction function X then follows from the relation (24).

Solution Procedure

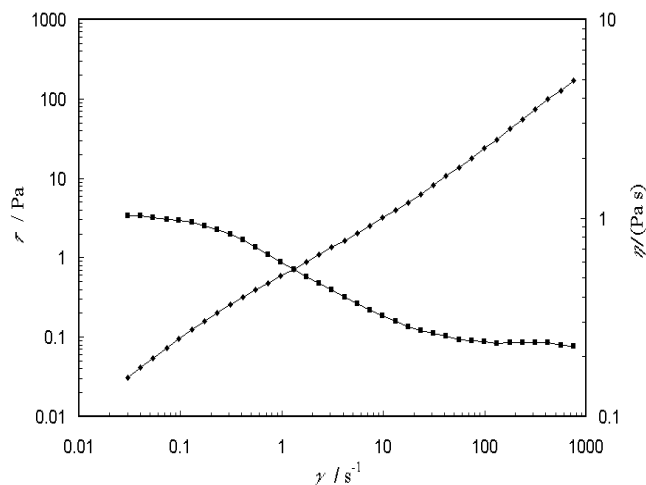
For numerical calculations of the upper bound X_u and the lower bound X_l special programs were compiled in Turbo Pascal. The calculations were performed for the varying values of quantities m , Λ , and η_r encompassing the intervals $0.3 \leq m \leq 1$ (with the step of 0.1), $0.1 \leq \Lambda \leq 2000$, and $0.5 \leq \eta_r \leq 1$ (with the step of 0.05).

The upper bound X_u was determined by minimization of the functional F_{ub} (eqn (13)) using the golden section method. The minimization was stopped when the relative deviation of the functional values at the end points of the varying interval of parameter a was lower than 0.5 %. The double integral included in eqn (13) (evaluated for each value of the parameter a) was calculated making use of the four-point Gauss formula. The quantity E_b , needed for the calculation of the integral, is given by eqn (15) as a function of II_b (eqns (19) and (23)).

The lower bound X_l was determined by maximization of the functional F_{lb} (eqn (25)). The procedures used for the optimization of parameter B and the double integral calculation were the same as in the case of

Table 1. Characteristics of the Test Liquids

| Symbol | Liquid | Density $\rho/(\text{kg m}^{-3})$ | Carreau model parameters | | | | |
|--------|-------------------------------|--------------------------------------|--------------------------|-----------------------------|--------------------|-------|----------|
| | | | $\eta_0/(\text{Pa s})$ | $\eta_\infty/(\text{Pa s})$ | λ/s | m | η_r |
| L1 | 25 % Emkarox, 0.06 % Praestol | 1043 | 1.00 | 0.21 | 3.6 | 0.442 | 0.790 |
| L2 | 25 % Emkarox, 0.08 % Praestol | 1043 | 1.65 | 0.27 | 5.5 | 0.432 | 0.836 |

**Fig. 1.** Example of the flow curve (\blacklozenge) and viscosity function (\blacksquare) courses for the liquid L2.

the upper bound estimation. The necessary quantity E_{cb} is given by eqn (26) as a function of II_b . The value of II_b was determined by the solution of the nonlinear eqn (27) using the Newton method. The iterations were stopped when the relative deviation of the two consecutive values of II_b was lower than 0.1 %.

EXPERIMENTAL

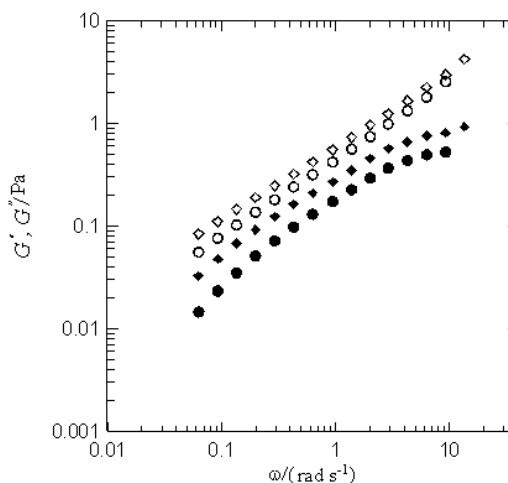
The experiments were directed to estimate the terminal falling velocities of spheres in aqueous solutions of polyalkylene glycol Emkarox HV 45 doped with a small amount (0.06 mass % and 0.08 mass %) of polyacrylamide Praestol 2935.

The test liquids were prepared by dissolving the corresponding amount of Praestol in 25 % aqueous solution of Emkarox HV 45. The viscosity measurements and the oscillation dynamic tests of liquids were carried out on rheometer RS 150 (Haake). The viscosity function courses were approximated by the Carreau model (1). The resulting values of model parameters of the liquids used are given in Table 1. An example of the flow and viscosity curves for the liquid L2 is shown in Fig. 1. In oscillatory tests, the comparable values of storage modulus G' and loss modulus G'' were found for both the liquids L1 and L2 as shown in Fig. 2. It suggests evident elasticity of the test liquids.

Seven types of glass spheres were used for drop tests. The diameter of spheres was measured with

Table 2. Characteristics of the Spherical Particles Used

| Symbol | Diameter, d/mm | Density, $\rho_s/(\text{kg m}^{-3})$ |
|--------|-------------------------|--------------------------------------|
| S1 | 1.46 ± 0.025 | 2464 ± 1.5 |
| S2 | 1.89 ± 0.045 | 2506 ± 1.6 |
| S3 | 2.50 ± 0.051 | 2516 ± 3.5 |
| S4 | 2.79 ± 0.035 | 2515 ± 3.1 |
| S5 | 3.13 ± 0.036 | 2463 ± 8.2 |
| S6 | 3.95 ± 0.049 | 2490 ± 2.0 |
| S7 | 4.92 ± 0.071 | 2514 ± 3.7 |

**Fig. 2.** Storage, G' (full symbols), and loss, G'' (empty symbols), moduli vs. angular velocity: liquid L1 (\diamond) and liquid L2 (\circ).

a micrometer. An average of twenty sphere measurements was used as the diameter. The density of spheres was measured using a pycnometer. Characteristics of the spheres used are given in Table 2.

Wall effects were accounted for by dropping each sphere in three Perspex columns of 20 mm, 40 mm, and 80 mm in diameter and about 0.8 m in length. The test section was situated nearly 0.2 m away from the top and bottom ends of the tube. The stopwatch reading to 0.01 s was used for timing the spheres. The timing was repeated 10 times for each type of spheres. The range of sphere velocities encountered in these measurements was from 1.32 mm s^{-1} to 28.2 mm s^{-1} . Corresponding intervals of Reynolds number and dimensionless time parameter were $0.002 \leq Re_{ct} \leq 0.420$ (creeping flow region) and $10 \leq \Lambda \leq 41$.

RESULTS AND DISCUSSION

Examples of the results of numerical calculations of upper and lower bounds to correction function X are given in Figs. 3–5 for $\eta_r = 1.0, 0.8,$ and 0.6 , respectively. The pseudoplasticity of a Carreau fluid increases with the increasing value of the model parameter λ and the decreasing value of parameter m . Accordingly, the values of X_u and X_l decrease as well with the increasing λ and decreasing m for a given value of viscosity parameter η_r . At the same time, the pseudoplasticity of a Carreau fluid goes down with decreasing η_r . Therefore, the smallest values of X_u and X_l for given λ and m were obtained for $\eta_r = 1$ and they increase with the decreasing η_r . Concerning the upper bound, $X_u \rightarrow 1$ for $\lambda \rightarrow 0$ and any m and η_r . It corresponds with Newtonian behaviour of the fluid at this condition. On the other hand, the lower bound $X_l \rightarrow 2/(1+m)$ for $\lambda \rightarrow 0$. Therefore, for low values of λ the more realistic estimation of the function X seems to be its upper bound X_u .

The results of the numerical calculations of the function X were compared with the experimental data X_{exp} calculated from the relationship

$$X_{\text{exp}} = \frac{g d^2 (\rho_s - \rho)}{18 \eta_0 u_t} \quad (31)$$

which follows for

$$F_d = \frac{4}{3} \pi R^3 (\rho_s - \rho) g \quad (32)$$

from eqns (10)–(12).

The values of u_t were determined for the fall of spheres S1–S7 in both test liquids L1 and L2 by linear extrapolation of the dependences of experimental values $u_{t,\text{exp}}$ on the ratio d/D to $d/D = 0$. The results are summarized along with the resulting values of X_{exp} in Table 3. At the same time, each value of $u_{t,\text{exp}}$ represents an average of ten measurements. Measurement error does not exceed 3 % in this case.

In Table 3 are given also the corresponding values of upper and lower bounds to X , which were calculated for the values of η_r , m , and λ characterizing the test liquids L1 and L2. It is evident that, unlike the experiments carried out in the presence of diluted aqueous solutions of only one polymer in which settling is dominated by the viscosity and viscoelastic influence is relatively small [5, 9], the values of X_{exp} are beyond the calculated interval of X_u and X_l being even higher than the upper bound X_u . At the same time, contrary to expectations, the value of X_{exp} (proportional to the drag coefficient) does not evidently decrease with the increasing value of λ . Therefore, the magnitude of relative deviation $\delta_u = (X_u - X_{\text{exp}})/X_{\text{exp}}$ between X_{exp} and X_u (Table 3) increases with increasing λ . The observed drag enhancement relative to a purely viscous

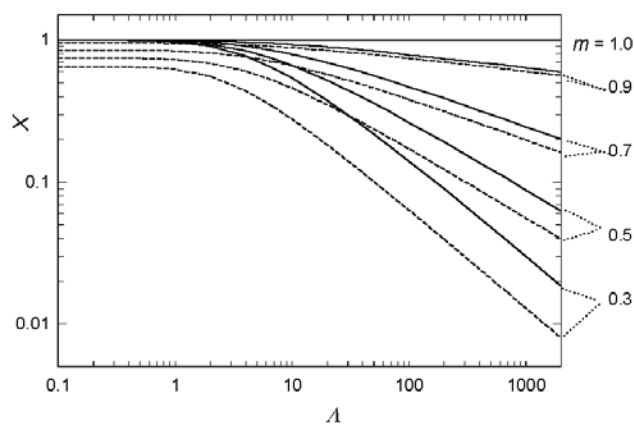


Fig. 3. Calculated values of the upper (solid line) and lower (dashed line) bounds to correction function X as a function of dimensionless time λ and parameter m for $\eta_r = 1$.

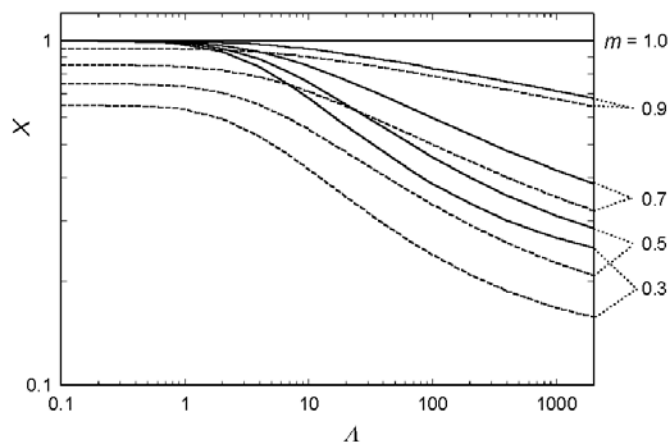


Fig. 4. Calculated values of the upper (solid line) and lower (dashed line) bounds to correction function X as a function of dimensionless time λ and parameter m for $\eta_r = 0.8$.

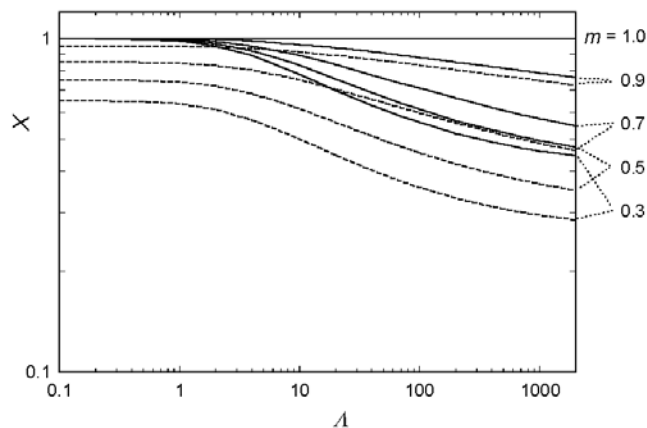


Fig. 5. Calculated values of the upper (solid line) and lower (dashed line) bounds to correction function X as a function of dimensionless time λ and parameter m for $\eta_r = 0.6$.

Table 3. Comparison of Experimental Values X_{exp} of Drag Coefficient Correction Function with Calculated Data of its Upper, X_u , and Lower, X_l , Bound

| Sphere | L1, $\eta_r = 0.79, m = 0.442$ | | | | | | L2, $\eta_r = 0.84, m = 0.432$ | | | | | |
|--------|--------------------------------|-----------------|-----------|-------|-------|-----------------|--------------------------------|-----------------|-----------|-------|-------|-----------------|
| | $u_t / (\text{mm s}^{-1})$ | Λ_{exp} | X_{exp} | X_u | X_l | $\delta_u / \%$ | $u_t / (\text{mm s}^{-1})$ | Λ_{exp} | X_{exp} | X_u | X_l | $\delta_u / \%$ |
| S1 | 2.08 | 10 | 0.793 | 0.739 | 0.517 | -6.8 | 1.32 | 10 | 0.758 | 0.712 | 0.529 | -6.0 |
| S2 | 3.86 | 15 | 0.737 | 0.676 | 0.471 | -8.3 | 2.54 | 15 | 0.679 | 0.640 | 0.441 | -5.4 |
| S3 | 6.48 | 18 | 0.770 | 0.649 | 0.452 | -15.7 | 4.03 | 18 | 0.751 | 0.613 | 0.420 | -18.4 |
| S4 | 8.33 | 21 | 0.747 | 0.626 | 0.436 | -16.2 | 5.18 | 20 | 0.729 | 0.596 | 0.408 | -18.2 |
| S5 | 10.4 | 24 | 0.728 | 0.607 | 0.423 | -16.6 | 6.21 | 22 | 0.740 | 0.581 | 0.398 | -21.5 |
| S6 | 16.8 | 30 | 0.732 | 0.577 | 0.401 | -21.2 | 10.4 | 29 | 0.718 | 0.540 | 0.369 | -24.7 |
| S7 | 28.2 | 41 | 0.688 | 0.537 | 0.374 | -22.0 | 15.9 | 35 | 0.740 | 0.514 | 0.351 | -30.6 |

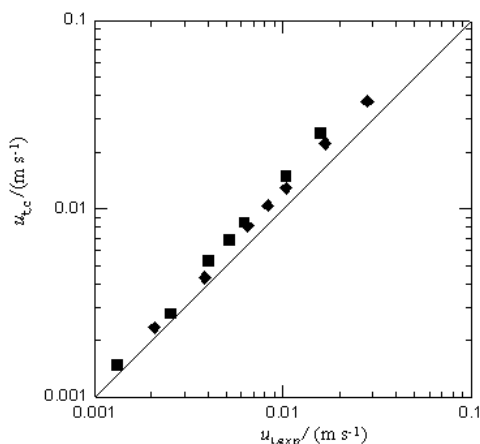


Fig. 6. Comparison of experimental terminal falling velocity data with those calculated according to eqns (31) and (33): liquid L1 (♦) and liquid L2 (■).

fluid will be apparently caused by intensified elastic effects at elevated dimensionless time Λ , as in the case of particles fall in Boger fluids (e.g. [10]).

It is evident that prediction of terminal falling velocity of spheres in test fluids is approximate only. The corresponding value of u_t is determined by eqn (31) substituting the upper bound X_u for X_{exp} . To do so, the dependences $X_u = X_u(\eta_r, m, \Lambda)$, calculated in this work (see Figs. 3–5), were approximated (mean relative deviation $\delta_u = 2.1 \%$) for the interval $0.5 \leq \eta_r \leq 0.95$ by the relationship

$$X_u = [1 + k_1(1 - m)\Lambda^2]^{k_2(1-m)k_3} \quad (33)$$

where

$$k_1 = 2.6 - 2.25\eta_r \quad (34a)$$

$$k_2 = -0.21 + 0.66\eta_r - 0.71\eta_r^2 \quad (34b)$$

$$k_3 = 0.054 + 0.54\eta_r \quad (34c)$$

Goodness of the fit of experimental terminal velocities by eqns (31) and (33) is shown in Fig. 6 for the test liquids L1 and L2.

The values of the relative deviations of experimental, $u_{t,exp}$, and calculated data, $u_{t,c}$, range from -12% to -59% . At the same time, in accordance with experimental values of X_{exp} , the magnitude of the deviation increases with increasing u_t .

It should be noted that due to the lack of terminal falling velocity experimental data for Carreau model liquids with $\eta_r < 0.96$ in the literature, the results obtained in this work could not be compared with those of other authors. For more comprehensive examination of the applicability of our numerical results for terminal falling velocity prediction, further experiments will be necessary in the wider intervals of parameters m and Λ .

Acknowledgements. The support of this study, performed in the framework of Grant Projects No. 104/03/0544 at the University of Pardubice, by the Grant Agency of the Czech Republic is gratefully appreciated.

SYMBOLS

| | | |
|-----------|---|--------------------|
| a | stream function parameter, eqn (23) | |
| B | shear stress function parameter, eqns (28), (29) | |
| c_D | sphere drag coefficient | |
| d | sphere diameter | m |
| D | test column diameter | m |
| E | function defined by eqn (16) | Pa s ⁻¹ |
| E_c | function defined in dimensionless form by eqn (26) | Pa s ⁻¹ |
| F | functionals, eqns (13), (25) | |
| F_d | drag force magnitude | N |
| g | gravity acceleration | m s ⁻² |
| m | Carreau model parameter | |
| R | sphere radius | m |
| p | pressure | Pa |
| r | radial spherical coordinate | m |
| Re_0 | Reynolds number defined by eqn (12) | |
| Re_{Ct} | Reynolds number based on the Carreau model viscosity for $\dot{\gamma} = u_t/d$ | |
| x | dimensionless radial spherical coordinate defined by eqn (14a) | |

| | | |
|--|---|----------------------------|
| X | drag coefficient correction function defined by eqn (11) | |
| y | dimensionless spherical coordinate defined by eqn (14b) | |
| u_i | velocity vector components | m s^{-1} |
| u_t | terminal falling velocity | m s^{-1} |
| δ | relative deviation | |
| η | non-Newtonian viscosity | Pa s |
| η_0 | Carreau model parameter (zero shear rate viscosity) | Pa s |
| η_r | dimensionless viscosity parameter defined by eqn (2) | |
| η_∞ | Carreau model parameter (infinity shear rate viscosity) | Pa s |
| θ | meridian spherical coordinate | |
| λ | Carreau model time parameter | s |
| Λ | dimensionless time parameter defined by eqn (18) | |
| ρ | liquid density | kg m^{-3} |
| ρ_s | sphere density | kg m^{-3} |
| $\dot{\gamma}$ | shear rate | s^{-1} |
| $\underline{\underline{\dot{\gamma}}}$ | shear rate tensor | s^{-1} |
| τ_{ij} | extra stress tensor components | Pa |
| $\underline{\underline{\tau}}$ | extra stress tensor | Pa |
| ψ | stream function, eqn (22) | $\text{m}^3 \text{s}^{-1}$ |
| II | second invariant of the shear rate tensor defined by eqn (6) | s^{-1} |
| II_τ | second invariant of the extra stress tensor given in dimensionless form by eqn (27) | Pa |

Superscripts

\rightarrow vector quantity

Subscripts

| | |
|--------------|--|
| b | dimensionless quantity |
| c | calculated |
| exp | experimental value |
| i, j | component |
| l | lower bound |
| r | related to the radial spherical coordinate |
| u | upper bound |
| θ | related to the meridian spherical coordinate |
| φ | related to the parallel spherical coordinate |

REFERENCES

1. Chhabra, R. P., *Bubbles, Drops, and Particles in Non-Newtonian Fluids*. CRC Press, Boca Raton, 1993.
2. Chhabra, R. P. and Uhlher, P. H. T., *Rheol. Acta* 19, 187 (1980).
3. Bush, M. B. and Phan-Tien, N., *J. Non-Newtonian Fluid Mech.* 16, 303 (1984).
4. Chhabra, R. P. and Dhingra, S. C., *Can. J. Chem. Eng.* 64, 897 (1986).
5. Doleček, P., Šiška, B., and Machač, I., *Sb. Věd. Prací, Vys. Škola Chem. Technol.* 54, 189 (1990), Pardubice (in Czech).
6. Machač, I., Doleček, P., Šiška, B., and Ulbrichová, I., *38th National CHISA Conference*, Seč, 1991 (in Czech).
7. Rektorys, K., *Variational Methods in Mathematics, Science and Engineering*. 2nd Edition. Reidel, Dordrecht—Boston, 1979.
8. Slattery, J. C., *Momentum, Energy, and Mass Transfer in Continua*. McGraw-Hill, New York, 1972.
9. Navez, V. and Walters, K., *J. Non-Newtonian Fluid Mech.* 67, 325 (1996).
10. Solomon, M. J. and Muller, S. J., *J. Non-Newtonian Fluid Mech.* 62, 81 (1996).